

Removal of humic acid from aqueous media using magnetite nanoparticles

Behzad Shahmoradi^{a,*}, Kitirote Wantala^b, H. Jari^a, Yahya Zandsalimi^a, S. Mohammadloo^a, Afshin Maleki^a, H.P. Shivaraju^c, Seok-Soon Choi^d, Seung-Mok Lee^{e,*}

^aDepartment of Environmental Health Engineering, Faculty of Health, Kurdistan University of Medical Sciences, Sanandaj, Iran, emails: bshahmorady@gmail.com/bshahmoradi@muk.ac.ir (B. Shahmoradi), hannahjari94@gmail.com (H. Jari), yzandsalimi@gmail.com (Y. Zandsalimi), salar.mhmdlo@gmail.com (S. Mohammadloo), maleki43@yahoo.com (A. Maleki)

^bDepartment of Chemical Engineering, Faculty of Engineering, Khon Kaen University, Khon Kaen, Thailand, email: kitirote@kku.ac.th (K. Wantala)

^cDepartment of Water and Health, Faculty of Life Sciences, JSS Academy of Higher Education and Research, Sri Shivarathreshwara Nagara, Mysuru – 570015, Karnataka, India, email: shivarajuenvi@gmail.com (H.P. Shivaraju)

^dDepartment of Biological and Environmental Engineering, Semyung University, Jecheon 27136, Republic of Korea, email: sschoi@semyung.ac.kr (S.-S. Choi)

^eDepartment of Health and Environment, Catholic Kwandong University, Gangnung 25601, Republic of Korea, email: leesm@cku.ac.kr (S.-M. Lee)

Received 7 April 2020; Accepted 6 September 2020

ABSTRACT

Humic acid is one of the predominant organic substances in both surface and ground waters, creating an unpleasant taste and color in water. It is one of the most important precursors of disinfection by-products. Magnetite nanoparticles were synthesized through the chemical precipitation method. Removal of humic acid from aqueous solutions using magnetite nanoparticles was compared with commercial hematite nanoparticles by changing the effective parameters including pH, nanoparticle dosage, humic acid concentration, reaction time, and temperature. Moreover, the adsorption isotherms were evaluated using Langmuir and Freundlich models. The results showed that by increasing pH from 3 to 11, the efficiency of both nanoparticles decreased. The highest performance of nanoparticles was achieved at pH = 3, nanoparticles dosage of 0.25 g/L, and contact time of 90 min. The isotherm graphs and linear regression coefficient values indicated that adsorption using hematite and magnetite fits the Langmuir models. The kinetic study showed that the adsorption using both hematite and magnetite follows second-order-kinetics. Both synthesized magnetite and commercial hematite show good performance for the removal of humic acid.

Keywords: Humic acid; Magnetite; Nanoparticles; Adsorption

1. Introduction

Natural organic matter (NOM) substances of biological and synthetic sources are important impurities that are present in all available aqueous sources. The presence of NOM affects the quality of water and it is problematic for

municipal wastewater treatment plants [1]. Humic substances are natural components of organic materials and are not only present in both surface and ground waters but also could be found abundantly in soils and sediments [2]. It is a major component of humic substances formed from the decomposition of plants and animal carcasses [3]. Humic

* Corresponding authors.

material has no definite chemical formula and has a number of functional groups; most of them are phenolic, carboxyl, carbonyl, and hydroxyl groups [4]. Humic acid causes an undesirable taste and color in water [5]; most importantly, they are the main precursors of disinfection byproducts such as trihalomethanes in drinking water formed in the chlorination process [6]. Due to the above mentioned and the threat to the environment and human health, it should be removed from the water contaminated.

Some methods to remove humic acid from aqueous media are coagulation [7], activated carbon adsorption [8], nano-TiO₂ photocatalysis [9], membrane filtration [10], and gas-phase surface discharge plasma system [11]. Each of these methods has certain advantages and disadvantages, for example, the concentration of metal ions in the coagulation process may be increased. In membrane filters, the limited size of the membrane is one of its problems. On the discharge plasma treatment, there is still no detailed report of its disinfection byproducts. Recently, some combination methods for the removal of humic substances have been developed such as ozonation–biofiltration process [12], coagulation process, and coagulation–ultrafiltration process [7]. In combination methods, the efficiency of removal is increased, but the disadvantages of any method are still present. On the other hand, adsorption in industrial processes is widely used, which is because of its high efficiency and cheapness compared with other methods [13]. Moreover, the adsorbents are easily collected from aqueous media [14] and are not sensitive to toxic substances [15].

Some adsorbents used for water treatment include activated carbon [16] and silica gel [17]. But these adsorbents are expensive, and researchers are trying to replace natural and cheap adsorbents, such as garden grass [18], sunflower leaves [19], egg shells [20], or green algae [21]. Fe₃O₄ nanoparticle is a common magnetic iron oxide that has a reverse cubic spinel structure with oxygen; it is usually produced by the co-precipitation of ferric and ferrous ions. The production of fine-size Fe₃O₄ particles and an acceptable size distribution without particle accumulation has been a constant problem [22]. For example, particle size smaller than 25 nm is formed by chemical co-precipitation [23], and the particle size greater than 50 nm with cube-octahedral morphologies was obtained by hydrolysis method [24]. In a study, modified Fe₃O₄ nanoparticles through chemical precipitation were used to remove methyl violet dye from aqueous media [25]. In another study, Fe₃O₄ nanoparticles were applied to remove As(III) and As(V) from aqueous solution. Iron oxide creates a strong reaction with arsenic [26]. Therefore, this paper was aimed at chemical synthesis of Fe₃O₄ nanoparticles and assessment its adsorption efficiency in removal of humic acid from aqueous media. It was compared with commercial hematite nanoparticles under different operational conditions for removal and economic efficiencies.

2. Materials and methods

2.1. Synthesis of magnetite nanoparticles

The Fe₂O₃ nanoparticles were purchased from Merck, Germany and used without any modification. The Fe₃O₄

nanoparticles were synthesized through co-precipitation method. In brief, 5.4 g FeCl₃·6H₂O and 2.78 g FeCl₂·4H₂O (>99%, Merck, Germany) with a weight ratio of 2:1 were mixed in a 100 mL conical flask and filled up with deionized water. The ammonia solution (25%, Merck, Germany) was added dropwise to the solution until the pH reached 9. Finally, a black-colored precipitate containing Fe₃O₄ nanoparticles was formed. The precipitate was stirred for 30 min and heated to 80°C. It was then washed three times using deionized water and washed twice with ethanol. The final product, black sediment containing Fe₃O₄ nanoparticles was separated from the solution using magnet [27].

2.2. Adsorption experiments

The effect of operational factors (pH, nanoparticle dosage, initial concentration of humic acid, reaction time, and temperature) on the adsorption efficiency was investigated by preparing 1,000 mg/L humic acid solution. 1 g/L solution of humic acid was prepared by dissolving 1 g of humic acid in 62.5 mL of 2 N NaOH making up to 1 L using distilled water. This solution was kept on magnetic stirrer for 48 h. The stock solution achieved was then kept at 4°C under darkness [28]. The desired pH (3, 5, 7, 9, and 11) was adjusted using 0.02N NaOH or HCl. The adsorption rate was determined by UV-vis spectrophotometer ($\lambda = 254$ nm).

2.2.1. Adsorption isotherms

Adsorption isotherm is one of the most important factors in designing adsorption systems. In fact, adsorption isotherm explains interactions between adsorbent and adsorbate [29]. One of the most general isotherms is single layer adsorption model proposed by Langmuir [30]. In Langmuir isotherm, it is supposed that adsorption happens in all homogenous sites and it is eventually applied for explaining single layer adsorption.

$$\frac{C_e}{q_e} = \frac{1}{q_m k_1} + \frac{1}{q_m} C_e \quad (1)$$

where C_e is the equilibrium concentration of anions in solution in mg/L, q_e is the concentration of adsorbed anions at the equilibrium time on the adsorbent in mg/g, q_m is the maximum adsorption capacity in mg/g, and k_1 is the Langmuir adsorption constant in L/mg. The suitability type of adsorption process in the Langmuir model can be determined using R_L dimensionless factors (Eq. (2)), so that $R_L > 1$ is undesirable adsorption, $R_L = 1$ is linear adsorption, $R_L = 0$ is irreversible adsorption, and $0 < R_L < 1$ is desired adsorption [31].

$$R_L = \frac{1}{1 + bC_0} \quad (2)$$

Another model is the multi-layer adsorption model expressed by Freundlich in 1906 [31]. The experimental equation of Freundlich isotherm (Eq. (3)) is based on the multi-layered, non-uniform, and heterogeneous adsorbent on the adsorbing material [32].

$$\log(q_e) = \log(K_F) + \frac{1}{n} \log(C_e) \quad (3)$$

where K_F and n are the Freundlich constants, which are dependent on the adsorption capacity and intensity; values of $n < 1$ indicates poor adsorption and values of 1–2, and 2–10 indicate average and desirable adsorption respectively.

2.2.2. Adsorption kinetics

The prediction of adsorption rate is one of the factors for designing an adsorption system. The kinetic equations are expressed in order to relatively estimate adsorption kinetics and mechanisms. In this study, the first-order (Eq. (4)) and pseudo-second-order (Eq. (5)) models were used to study the adsorption mechanism.

$$\ln(q_e - q_t) = \ln(q_e) - k_1 t \quad (4)$$

$$\frac{t}{q_t} = \frac{1}{k_2 q_e^2} + \frac{1}{q_e} t \quad (5)$$

where k_1 and k_2 are the coefficient of speed (1/min) and second-order reaction constant (g/mg min), q_e and q_t are the adsorption capacity at the time of equilibrium and the adsorption capacity at time t (mg/g), respectively.

3. Results and discussion

3.1. Nanoparticle characterization

The X-ray diffraction (XRD) patterns of hematite and magnetite nanoparticles are shown in Fig. 1. The appearance of peaks at $2\theta = 19.54^\circ, 30.50^\circ, 35.61^\circ, 43.43^\circ, 54.11^\circ, 57.51^\circ, 63.06^\circ,$ and 74.58° with corresponding to diffraction indices of (111), (220), (311), (222), (400), (422), (511), and (440) are characteristic peaks of cubic structure of magnetite [33]. The sharpness and high intensity of the peaks confirm the good crystallinity nature of the nanoparticles fabricated [34]. The Fourier transform infrared (FTIR) spectra of hematite and magnetite nanoparticles were recorded in the range of 400–4,000 cm^{-1} wavenumber, identifying the chemical bonds and the corresponding functional groups. As depicted in Fig. 2, the large broad bands at 3,928; 3,551; and 3,417 cm^{-1} are ascribed to the O–H stretching vibration of OH groups [35]. The absorption peaks around 1,618 and 1,637 cm^{-1} are due to the asymmetric and symmetric bending vibration of C=O. The strong band below 625 cm^{-1} is assigned to Fe–O stretching mode. However, there is negligible difference in the functional groups available on hematite and magnetite. The reason could be attributed to the fact that no organic compound was used for preparation of these nanoparticles. Fig. 3 shows the scanning electron microscopy (SEM) images of hematite and magnetite nanoparticles. The morphology of the nanoparticles is quasi-spherical and there is no obvious difference in changing morphology, indicating the independence of the nanoparticles. Moreover, the agglomerated nanoparticles could be attributed to the high specific surface area resulting in high surface energy [36].

3.2. Adsorption studies

3.2.1. Effect of pH

pH is one of the factors that affects the adsorbent surface load and affects the process efficiency [37]. According to Fig. 4, it is shown that the removal efficiency is high at low pH and the performance of the nanoparticle is better in removing the humic acid. On the other hand, by increasing the pH, the removal efficiency, and the capacity for the adsorption of humic acid is reduced. The removal efficiency of humic acid by magnetite was 80% and 35% at pH = 3 and 11, respectively. Under alkaline conditions, $\text{Fe}(\text{OH})_3$ is formed and reduces the reaction speed. Moreover, the pK_a values of acidic sites on various humic substances are generally in the range of 3–4.5. Therefore, if the solution has pH larger than these pK_a values, phenolic and carboxylic groups in the humic acid structure are ionized and humic acid becomes dominantly negatively charged. Hence, electrostatic attraction between surfaces positive charge on nanoparticles and surface negative charge of humic acid increases, so the highest extents of humic acid uptake was obtained at pH=3 [38].

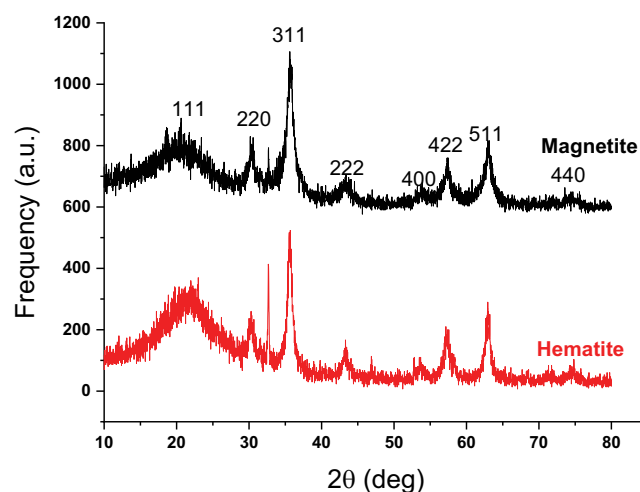


Fig. 1. XRD patterns of hematite and magnetite nanoparticle.

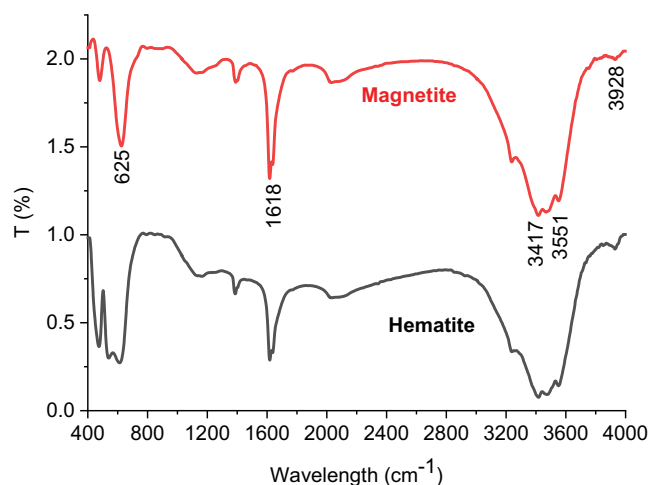


Fig. 2. FTIR spectra of hematite and magnetite nanoparticle.

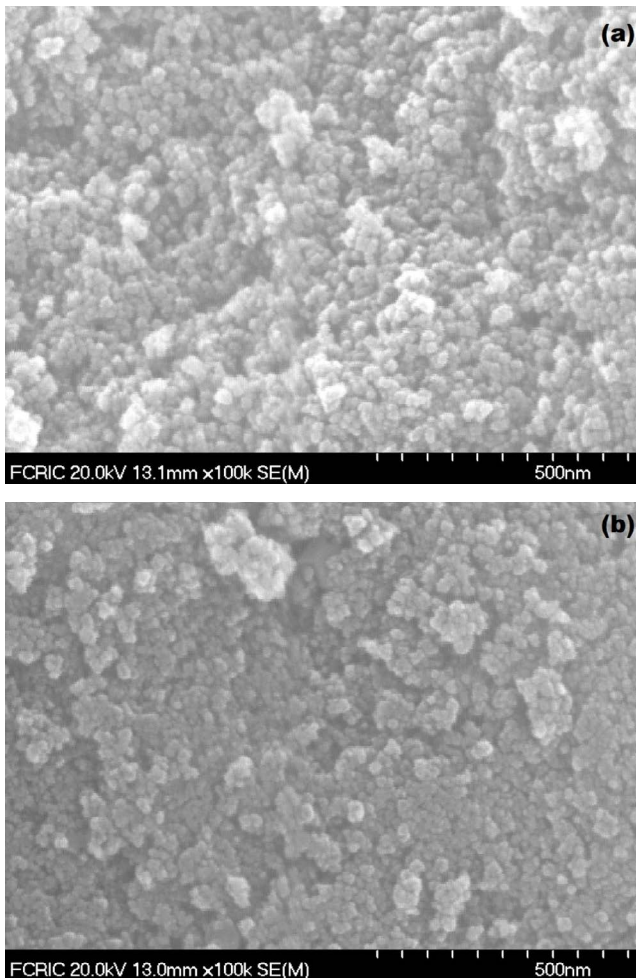


Fig. 3. SEM images of (a) hematite and (b) magnetite nanoparticle.

3.2.2. Effect of contact time

The effect of contact time on the removal efficiency of humic acid (100 mg/L) was investigated using nanoparticles (0.25 g/L) at pH = 3. The results are presented in Fig. 5. It is evident from Fig. 5 that increasing the contact time for both nanoparticles increases the removal efficiency of humic acid so that for hematite, at 15 min, the adsorption efficiency was 19.15%, while it becomes 71.49% after 90 min. For magnetite, the absorption efficiency was 1.14% at 15 min, while it increased to 99.67% at 90 min. This indicates that over time, the surface becomes less accessible, and thus the rate of adsorption decreases [39]. However, as it is depicted in Fig. 5, the adsorption was almost constant from 60 to 90 min. Hence, the optimum contact time was considered as 60 min for the rest of the experiments.

3.2.3. Effect of adsorbent dosage

Detection of adsorbent doses due to economic problems is one of the most important issues in adsorption systems. Increasing the adsorbent dose provides a higher level of adsorption [40]. The contact between the pollutant and

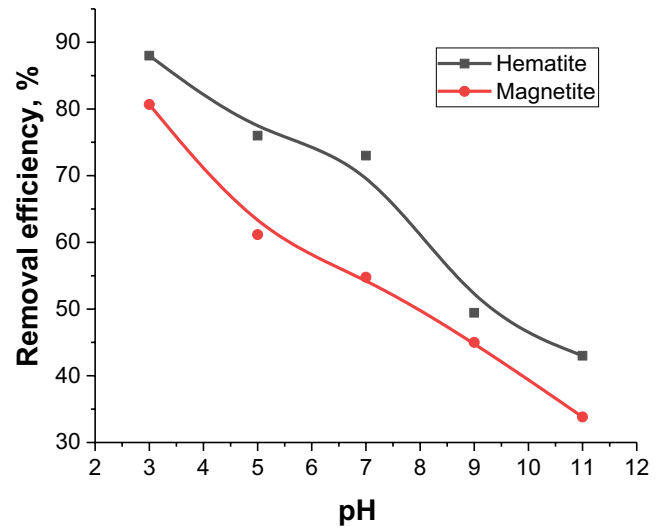


Fig. 4. Effect of pH on the efficiency of removal of humic acid using magnetite and hematite nanoparticles (humic acid concentration = 20 mg/L, adsorbent dosage = 0.15 g/L, and contact time = 60 min).

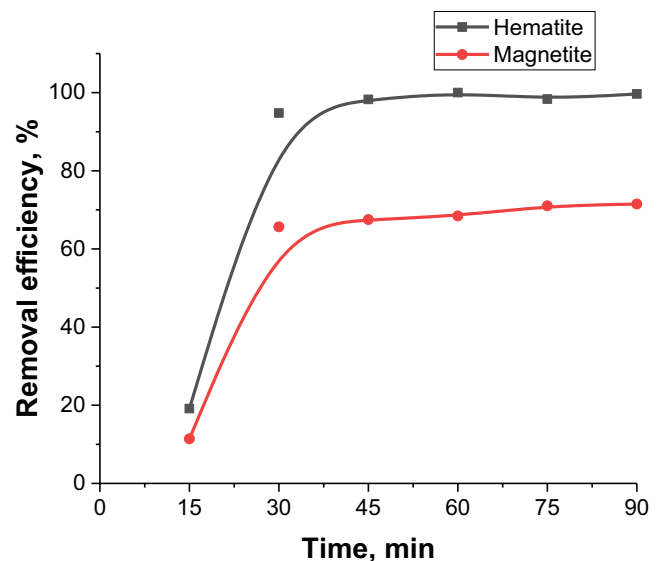


Fig. 5. Effect of contact time on the removal efficiency of humic acid using magnetite and hematite nanoparticles (adsorbent dosage = 0.25 g/L, humic acid concentration = 100 mg/L, and pH = 3).

the adsorbent increases the removal efficiency and causes a higher percentage of humic acid to be removed [41]. As shown in Fig. 6, the efficiency of removal is increased by increasing the adsorbent dose. In the case of hematite, increasing the amount of adsorbent dose after a while, the tilt of the removal becomes milder. However, in magnetite, with increased adsorbent dose, the removal efficiency is much higher. The removal efficiency at a dose of 0.025 g/L was 63.37% and 12.18% for hematite and magnetite, respectively. Whereas, increasing the dose to 0.25 g/L resulted in increasing removal efficiency to 79.10% and 98.32% for hematite and

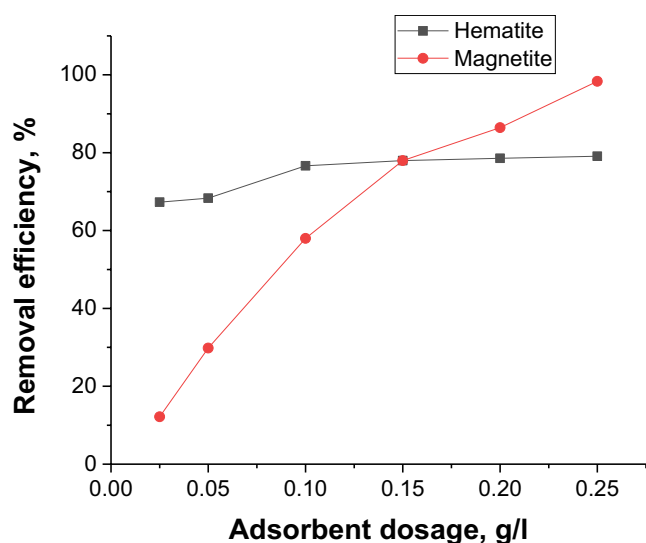


Fig. 6. Effect of adsorbent dose on the efficiency of removal of humic acid from water (humic acid concentration = 0.25 mg/L, pH = 3, and contact time = 60 min).

magnetite, respectively. On the other hand, although hematite initially showed higher adsorption efficiency but with increasing adsorbent dosage, magnetite showed superiority in adsorption efficiency. Studies done by Tang and Lo [42] showed that with the increase in the dosage of iron nanoparticles, the efficiency of removal of dye increased.

3.2.4. Effect of humic acid concentration

In Fig. 7, the effectiveness of both adsorbents in various concentrations of humic acid (10–200 mg/L) was investigated. In both nanoparticles, by increasing the concentration of humic acid, the adsorption efficiency decreased. However, the superiority of hematite was observed when its adsorption efficiency was slightly decreased from 100% to 87.5% when the humic acid concentration was increased from 10 to 200 mg/L, whereas, this adsorption efficiency for magnetite under the same conditions reduced from 79% to 33.7%. It could be attributed to the ratio between the number of pollutant molecules and the active surface absorbed therein. When the number of pollutant molecules was increased in the adsorption reaction environment, the efficiency was decreased [43].

3.2.5. Effect of temperature

The effect of temperature on the efficiency of removal of humic acid was investigated at three different temperatures for both adsorbents. The removal efficiency was investigated for each temperature at three concentrations. Based on Fig. 8, for both adsorbents, the efficiency decreased with increasing temperature; the decrease had less slope in the case of hematite.

3.2.6. Adsorption isotherms

For isotherm assessment, different concentrations of humic acid (10–150 mg/L) at pH = 3 at different temperatures

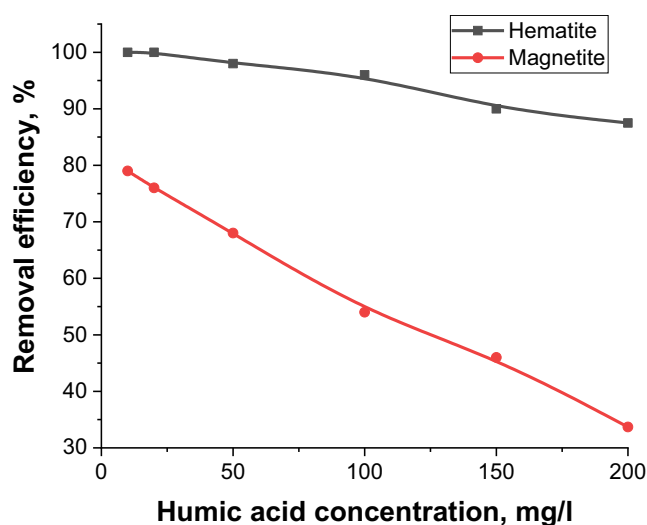


Fig. 7. Effect of humic acid concentration on its removal efficiency using magnetite and hematite nanoparticles (adsorbent dosage = 0.1 g/L, pH = 3, and contact time = 60 min).

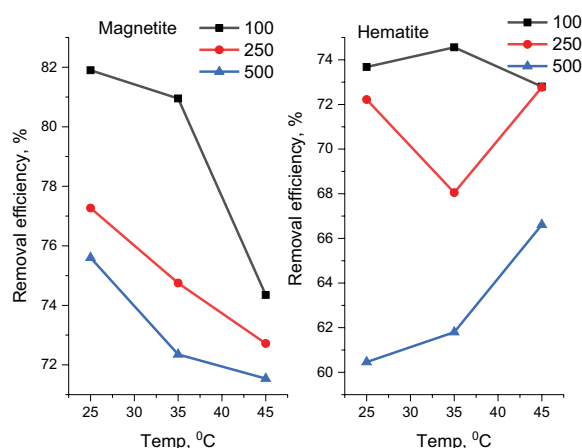


Fig. 8. Effect of temperature on the removal efficiency of humic acid (adsorbent dosage = 0.1 g/L, pH = 3, contact time = 60 min, and humic acid concentration of 100–500 mg/L).

(25°C, 35°C, and 45°C) were evaluated. Figs. 9 and 10 show the adsorption isotherms using Langmuir and Freundlich isotherm models. According to isotherm graphs shown in Figs. 9 and 10, linear regression coefficients for hematite ($R^2 = 0.8914$) and magnetite ($R^2 = 0.9504$) with the Langmuir model was more suitable compared with the Freundlich model for which the regression coefficient was $R^2 = 0.6425$ (hematite) and $R^2 = 0.8911$ (magnetite). Studying adsorption kinetics and thermodynamic of RY4 dye, it was reported that the adsorption isotherm follows the Langmuir model [44].

3.2.7. Adsorption kinetic of humic acid

For this purpose, the adsorption study was carried out using 0.25 g/L of nanoparticles, 100 mg/L of humic acid at pH = 3 for 15, 30, 45, 60, 75, and 90 min. After calculating the removal efficiency, the adsorption constants were

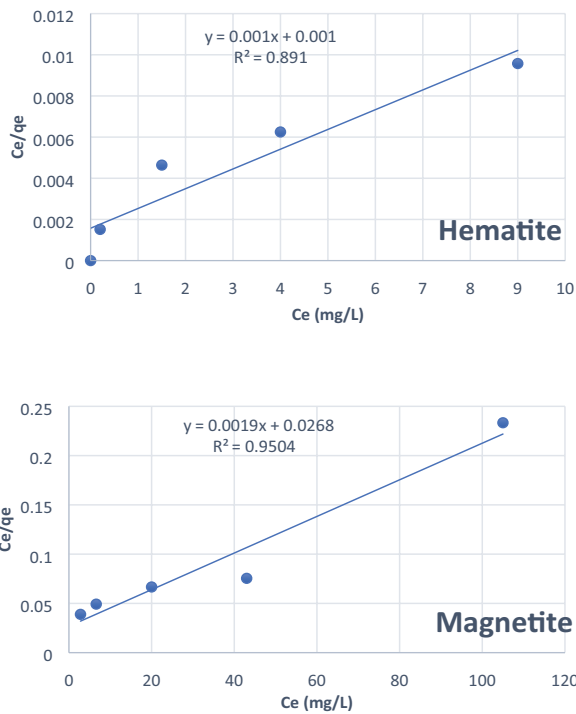


Fig. 9. Langmuir isotherm model for adsorption of humic acid using hematite and magnetite nanoparticles.

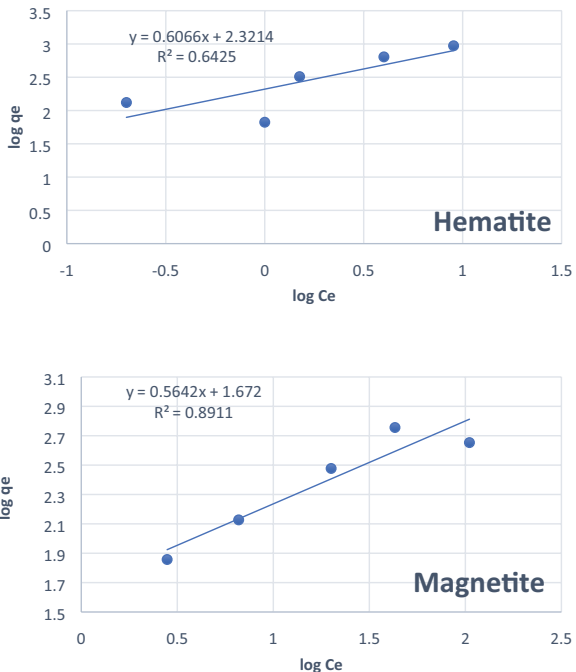


Fig. 10. Freundlich isotherm model for adsorption of humic acid using hematite and magnetite nanoparticles.

measured using first and second-order models (Figs. 11 and 12). It was found that both hematite and magnetite adsorbents follow second-order reaction. The study of Gao et al. [45] showed that the adsorption kinetic with $R^2 = 0.9998$

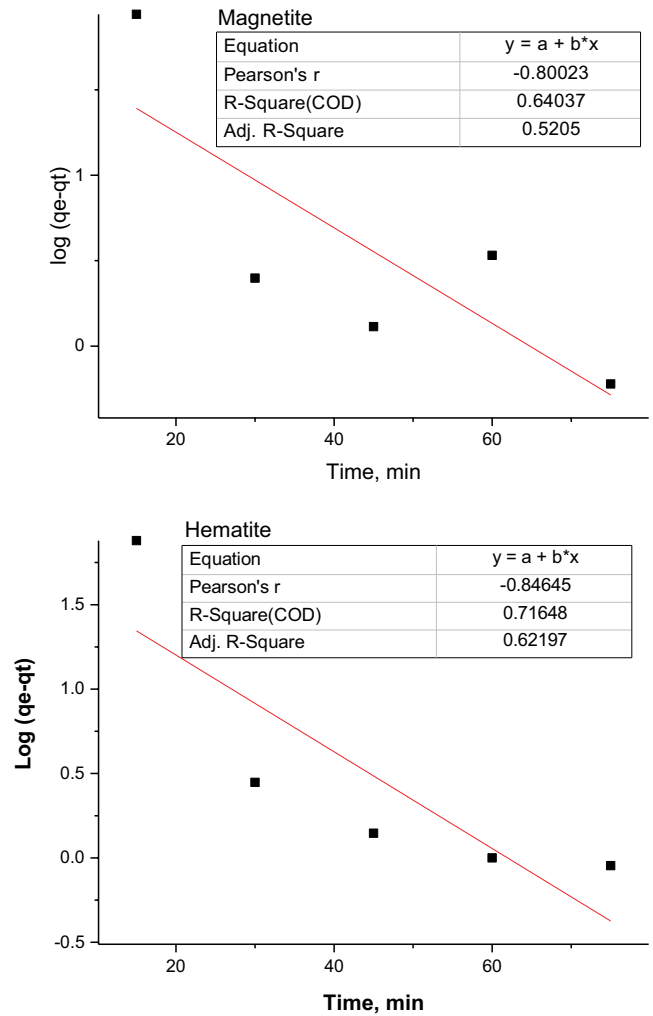


Fig. 11. First-order adsorption kinetic (humic acid concentration = 100 mg/L, nanoparticles dosage = 0.25 g/L, and pH = 3).

corresponds to the pseudo-second-order equation and is consistent with the present study.

4. Conclusions

In this study, the adsorption of humic acid was investigated using magnetite and hematite nanoparticles. The nanoparticles were characterized by the XRD analysis that confirmed the good crystallinity nature of the nanoparticles fabricated. The FTIR spectra of hematite and magnetite nanoparticles were recorded in the range if 400–4,000 cm^{-1} wavenumber, identifying the chemical bonds and the corresponding functional groups. The SEM images show that the morphology of the nanoparticles is quasi-spherical and there is no obvious difference in changing morphology, indicating the independency of the nanoparticles. This study found that both commercial hematite and the synthesized magnetite nanoparticles have good adsorption properties. It was found that acidic conditions (pH = 3) favors the adsorption condition. The nanoparticles could adsorb up to 200 mg/L humic acid at dosage of 0.25 g/L. However, the

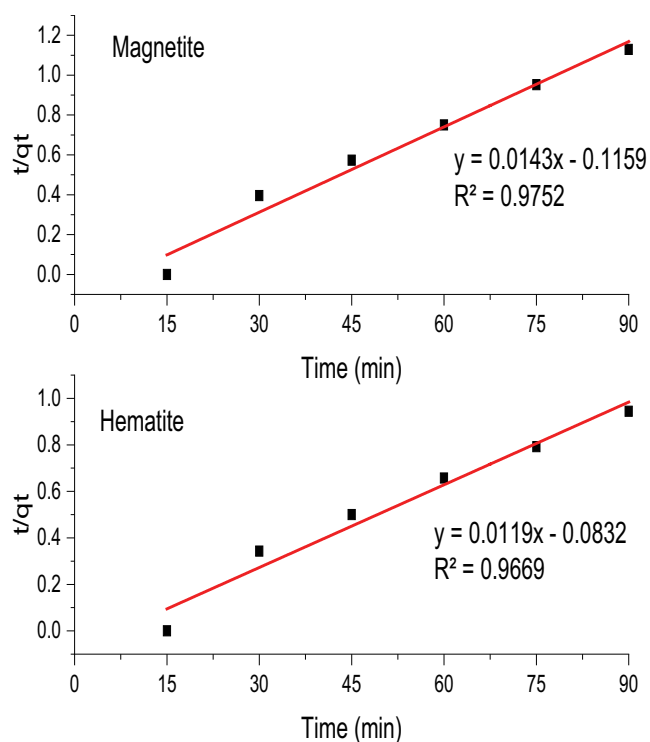


Fig. 12. Second-order adsorption kinetic (humic acid concentration = 100 mg/L, nanoparticles dosage = 0.25 g/L, and pH = 3).

commercial hematite was much more effective at higher pollutant concentration compared with magnetite nanoparticles synthesized. On the other hand, for higher concentration of humic acid, magnetite is recommended and hematite is suggested at beyond this limit. Both nanoparticles followed second-order-kinetic, fitted the Langmuir isotherm model and showed good performance for removal of humic acid.

Acknowledgments

The authors would like to thank Kurdistan University of Medical Sciences, Sanandaj, Iran for providing financial supports under Grant Number: 1396/52. This research was also supported by Basic Science Research Program through the National Research Foundation of Korea (NRF) funded by the Ministry of Education (NRF-2019R1I1A3A01062424). This study was also partially supported by International Affairs Division of Khon Kaen University (International Visiting Scholar, 2019 for Assoc. Prof. Behzad Shahmoradi).

References

- [1] V. Oskoei, M. Dehghani, S. Nazmara, B. Heibati, M. Asif, L. Tyagi, S. Agarwal, V.L. Gupta, Removal of humic acid from aqueous solution using UV/ZnO nano-photocatalysis and adsorption, *J. Mol. Liq.*, 213 (2016) 374–380.
- [2] M. Brum, J.F. Oliveira, Removal of humic acid from water by precipitate flotation using cationic surfactants, *Miner. Eng.*, 20 (2007) 945–949.
- [3] T. Wang, G. Qu, J. Ren, Q. Yan, Q. Sun, D. Liang, S. Hu, Evaluation of the potentials of humic acid removal in water by gas phase surface discharge plasma, *Water Res.*, 89 (2016) 28–38.
- [4] X. Qin, F. Liu, G. Wang, G. Huang, Adsorption of humic acid from aqueous solution by hematite: effects of pH and ionic strength, *Environ. Earth Sci.*, 73 (2015) 4011–4017.
- [5] L. Pinheiro, R. Pelegrini, R. Bertazzoli, A. Motheo, Photoelectrochemical degradation of humic acid on a (TiO₂)_{0.7}(RuO₂)_{0.3} dimensionally stable anode, *Appl. Catal., B*, 57 (2015) 75–81.
- [6] M.-C. Wei, K.-S. Wang, T.-E. Hsiao, L.-C. Lin, H.-J. Wu, Y.-L. Wu, P.-H. Liu, S.-H. Chang, Effects of UV irradiation on humic acid removal by ozonation, Fenton and Fe⁰/air treatment: THMFP and biotoxicity evaluation, *J. Hazard. Mater.*, 195 (2011) 324–331.
- [7] Y. Wang, Q. Wang, B.-Y. Gao, Q. Yue, Y. Zhao, The disinfection by-products precursors removal efficiency and the subsequent effects on chlorine decay for humic acid synthetic water treated by coagulation process and coagulation-ultrafiltration process, *Chem. Eng. J.*, 193 (2012) 59–67.
- [8] M.S. Rauthula, V.C. Srivastava, Studies on adsorption/desorption of nitrobenzene and humic acid onto/from activated carbon, *Chem. Eng. J.*, 168 (2011) 35–43.
- [9] S. Liu, M. Lim, R. Fabris, C. Chow, K. Chiang, M. Drikas, R. Amal, Removal of humic acid using TiO₂ photocatalytic process-fractionation and molecular weight characterisation studies, *Chemosphere*, 72 (2008) 263–271.
- [10] P.D. Peeva, A.E. Palupi, M. Ulbricht, Ultrafiltration of humic acid solutions through unmodified and surface functionalized low-fouling polyethersulfone membranes—effects of feed properties, molecular weight cut-off and membrane chemistry on fouling behavior and cleanability, *Sep. Purif. Technol.*, 81 (2011) 124–133.
- [11] Q. Zhang, G. Qu, T. Wang, C. Li, H. Qiang, Q. Sun, D. Liang, S. Hu, Humic acid removal from micro-polluted source water in the presence of inorganic salts in a gas-phase surface discharge plasma system, *Sep. Purif. Technol.*, 187 (2017) 334–342.
- [12] B. Seredyńska-Sobecka, M. Tomaszewska, A.W. Morawski, Removal of humic acids by the ozonation-biofiltration process, *Desalination*, 198 (2006) 265–273.
- [13] L. Peng, P. Qin, M. Lei, Q. Zeng, H. Song, J. Yang, J. Shao, B. Liao, J. Gu, Modifying Fe₃O₄ nanoparticles with humic acid for removal of Rhodamine B in water, *J. Hazard. Mater.*, 209 (2012) 193–198.
- [14] Y. Lin, H. Chen, K. Lin, B. Chen, C. Chiou, Application of magnetic particles modified with amino groups to adsorb copper ions in aqueous solution, *J. Environ. Sci.*, 23 (2011) 44–50.
- [15] D. Mehta, S. Mazumdar, S. Singh, Magnetic adsorbents for the treatment of water/wastewater—a review, *J. Water Process Eng.*, 7 (2015) 244–265.
- [16] F. Di Natale, A. Erto, A. Lancia, Desorption of arsenic from exhaust activated carbons used for water purification, *J. Hazard. Mater.*, 260 (2013) 451–458.
- [17] P. Yin, Q. Xu, R. Qu, G. Zhao, Removal of transition metal ions from aqueous solutions by adsorption onto a novel silica gel matrix composite adsorbent, *J. Hazard. Mater.*, 169 (2009) 228–232.
- [18] M. Hossain, H. Ngo, W. Guo, T. Setiadi, Adsorption and desorption of copper(II) ions onto garden grass, *Bioresour. Technol.*, 121 (2012) 386–395.
- [19] H. Benaissa, M. Elouchdi, Removal of copper ions from aqueous solutions by dried sunflower leaves, *Chem. Eng. Process. Process Intensif.*, 46 (2007) 614–622.
- [20] D. Podstawczyk, A. Witek-Krowiak, K. Chojnacka, Z. Sadowski, Biosorption of malachite green by eggshells: mechanism identification and process optimization, *Bioresour. Technol.*, 160 (2014) 161–165.
- [21] E. Bakatula, E. Cukrowska, L. Weiersbye, I. Mihaly-Cozmuta, A. Peter, H. Tutu, Biosorption of trace elements from aqueous systems in gold mining sites by the filamentous green algae (*Oedogonium* sp.), *J. Geochem. Explor.*, 144 (2014) 492–503.
- [22] S. Sun, H. Zeng, Size-controlled synthesis of magnetite nanoparticles, *J. Am. Chem. Soc.*, 124 (2002) 8204–8205.
- [23] X. Liu, M.D. Kaminski, Y. Guan, H. Chen, H. Liu, A.J. Rosengart, Preparation and characterization of hydrophobic superparamagnetic magnetite gel, *J. Magn. Mater.*, 306 (2006) 248–253.

- [24] J. Mürbe, A. Rechtenbach, J. Töpfer, Synthesis and physical characterization of magnetite nanoparticles for biomedical applications, *Mater. Chem. Phys.*, 110 (2008) 426–433.
- [25] F. Keyhanian, S. Shariati, M. Faraji, M. Hesabi, Magnetite nanoparticles with surface modification for removal of methyl violet from aqueous solutions, *Arabian J. Chem.*, 9 (2016) S348–S354.
- [26] J. Mayo, C. Yavuz, S. Yean, L. Cong, H. Shipley, W. Yu, J. Falkner, A. Kan, M. Tomson, V. Colvin, The effect of nanocrystalline magnetite size on arsenic removal, *Sci. Technol. Adv. Mater.*, 8 (2007) 71–75.
- [27] Z. Yuanbi, Q. Zumin, J. Huang, Preparation and analysis of Fe_3O_4 magnetic nanoparticles used as targeted-drug carriers, *Chin. J. Chem. Eng.*, 16 (2008) 451–455.
- [28] E. Bazrafshan, H. Biglari, A.H. Mahvi, Humic acid removal from aqueous environments by electrocoagulation process using iron electrodes, *J. Chem.*, 9 (2012) 2453–2461.
- [29] K. Yaghmaeian, N. Jaafarzadeh, R. Nabizadeh, H. Rasoulzadeh, B. Akbarpour, Evaluating the performance of modified adsorbent of zero valent iron nanoparticles–chitosan composite for arsenate removal from aqueous solutions, *Iran. J. Health Environ.*, 8 (2016) 535–548.
- [30] I. Langmuir, The adsorption of gases on plane surfaces of glass, mica and platinum, *J. Am. Chem. Soc.*, 40 (1918) 1361–1403.
- [31] H. Freundlich, Über die adsorption in lösungen, *Z. Phys. Chem.*, 57 (1907) 385–470.
- [32] V. Vimonses, S. Lei, B. Jin, C.W. Chow, C. Saint, Kinetic study and equilibrium isotherm analysis of Congo Red adsorption by clay materials, *Chem. Eng. J.*, 148 (2009) 354–364.
- [33] M.A. Vargas, J.E. Diosa, E. Mosquera, Data on study of hematite nanoparticles obtained from iron(III) oxide by the Pechini method, *Data Brief*, 25 (2019), doi: 10.1016/j.dib.2019.104183.
- [34] K.K. Kefeni, T.A. Msagati, T.T. Nkambule, B.B. Mamba, Synthesis and application of hematite nanoparticles for acid mine drainage treatment, *J. Environ. Chem. Eng.*, 6 (2018) 1865–1874.
- [35] A. Miri, M. Khatami, M. Sarani, Biosynthesis, magnetic and cytotoxic studies of hematite nanoparticles, *J. Inorg. Organomet. Polym. Mater.*, 30 (2020) 767–774.
- [36] V. Silva, P. Andrade, M. Silva, L.D.L.S. Valladares, J.A. Aguiar, Synthesis and characterization of Fe_3O_4 nanoparticles coated with fucan polysaccharides, *J. Magn. Magn. Mater.*, 343 (2013) 138–143.
- [37] J. Safari, Z. Zarnegar, M. Heydarian, Magnetic Fe_3O_4 nanoparticles as efficient and reusable catalyst for the green synthesis of 2-amino-4 h-chromene in aqueous media, *Bull. Chem. Soc. Jpn.*, 85 (2012) 1332–1338.
- [38] H. Esmaili, A. Ebrahimi, M. Hajian, H.R. Pourzamani, Kinetic and isotherm studies of humic acid adsorption onto iron oxide magnetic nanoparticles in aqueous solutions, *Int. J. Environ. Health Eng.*, 1 (2012), doi: 10.4103/2277-9183.100133.
- [39] M. Kilianová, R. Pucek, J. Filip, J. Kolařík, L. Kvítek, A. Panáček, J. Tuček, R. Zbořil, Remarkable efficiency of ultrafine superparamagnetic iron(III) oxide nanoparticles toward arsenate removal from aqueous environment, *Chemosphere*, 93 (2013) 2690–2697.
- [40] B. Shahmoradi, A. Maleki, K. Byrappa, Removal of disperse orange 25 using *in situ* surface-modified iron-doped TiO_2 nanoparticles, *Desal. Water Treat.*, 53 (2015) 3615–3622.
- [41] E. Bazrafshan, A.A. Zarei, H. Nadi, M.A. Zazouli, Adsorptive removal of methyl orange and reactive red 198 dyes by moringa peregrina ash, *Indian J. Chem. Technol.*, 21 (2014) 105–113.
- [42] S.C. Tang, I.M. Lo, Magnetic nanoparticles: essential factors for sustainable environmental applications, *Water Res.*, 47 (2013) 2613–2632.
- [43] H.-Y. Shu, M.-C. Chang, H.-H. Yu, W.-H. Chen, Reduction of an azo dye Acid Black 24 solution using synthesized nanoscale zerovalent iron particles, *J. Colloid Interface Sci.*, 314 (2007) 89–97.
- [44] A. Afkhami, R. Norooz-Asl, Removal, preconcentration and determination of Mo(VI) from water and wastewater samples using maghemite nanoparticles, *Colloids Surf., A*, 346 (2009) 52–57.
- [45] H. Gao, T. Kan, S. Zhao, Y. Qian, X. Cheng, W. Wu, X. Wang, L. Zheng, Removal of anionic azo dyes from aqueous solution by functional ionic liquid cross-linked polymer, *J. Hazard. Mater.*, 261 (2013) 83–90.